

Photoluminescence and photoluminescence excitation spectroscopy of multiple Nd^{3+} sites in Nd-implanted GaN

S. Kim, S. J. Rhee, X. Li, J. J. Coleman, and S. G. Bishop

Microelectronics Laboratory, University of Illinois at Urbana-Champaign, Urbana, Illinois 61801

(Received 5 January 1998)

Site-selective photoluminescence (PL) and photoluminescence excitation (PLE) spectroscopies were carried out at 6 K on the Nd^{3+} emissions from the ${}^4F_{3/2} \rightarrow {}^4I_{11/2}$ transition in Nd-implanted GaN grown by metal-organic chemical-vapor deposition. A detailed investigation of the Nd^{3+} PL spectra excited by selected wavelengths of above-gap and below-gap pump light has detected multiple, distinct ${}^4F_{3/2} \rightarrow {}^4I_{11/2}$ Nd^{3+} emission spectra characteristic of five different Nd^{3+} sites in the Nd-implanted GaN. The site-selective PLE spectra detected at emission wavelengths characteristic of each of these distinct Nd^{3+} PL bands include spectral features representative of excitation by above-gap absorption, by direct sharp-line Nd^{3+} 4*f*-shell absorption, and by broad, below-gap absorption bands attributable to defects and impurities and a possible isoelectronic trap associated with one of the five Nd^{3+} sites. It is concluded that the Nd^{3+} site that is excited by direct sharp-line Nd^{3+} 4*f*-shell absorption is the dominant or highest concentration Nd^{3+} center. The excitation mechanisms for the other four Nd^{3+} sites all involve the nonradiative transfer of energy from impurity- or defect-related traps to neighboring rare-earth atoms. These multiple excitation mechanisms closely parallel those observed previously in the PLE studies of GaN:Er. The similarities and relationships between the Nd^{3+} and Er^{3+} PL and PLE spectra in GaN, and the implications for the trap-mediated excitation mechanisms, are discussed. [S0163-1829(98)03323-2]

Several photoluminescence (PL) investigations of intra-4*f*-shell emissions from implanted rare-earth (RE) ions in crystalline semiconductors have demonstrated that the implanted RE ions can occupy multiple, distinct sites in the crystal.¹⁻⁷ Each of these rare earth sites is characterized by a different crystal field, which causes changes in the spectral distribution of the 4*f* band emissions from the rare earths that enable the different sites to be distinguished on the basis of their PL spectra.

Different rare-earth sites can be selectively excited by proper choice of pump wavelength. In some cases, this involves the selection of a specific intra-4*f*-shell absorption line with a tunable laser.¹ This type of wavelength-selective excitation occurs only for RE centers or sites that are present in relatively high concentrations because the optical-absorption cross section for direct intra-4*f*-shell absorption by RE atoms is quite small. In recently reported PL and photoluminescence excitation (PLE) studies of Er-implanted GaN, we observed site-selective excitation of Er^{3+} emission from four distinct sites,⁴⁻⁷ only one of which was pumped by direct 4*f*-shell absorption. Excitation of the other three Er^{3+} sites involved wavelength-selective pumping into broad, below-gap absorption bands attributable to defects or background impurities, with subsequent nonradiative transfer of the energy to nearby Er^{3+} luminescence centers. Furthermore, we were able to distinguish broadband, below-gap optical excitation processes for Er^{3+} emission that are attributable to (1) absorption due to implantation damage-induced defects, (2) absorption due to defects or impurities characteristic of the as-grown GaN film, and (3) an Er-specific absorption band just below the band gap which may involve the formation of an Er-related isoelectronic trap.⁷ The two sites excited by impurity- or defect-related absorption bands are

also strongly pumped by above-gap optical absorption (sometimes referred to as "host excitation"),^{1,5} while the sites pumped by the Er-related trap and direct 4*f*-shell absorption are not.

In order to determine whether our observations and conclusions regarding the excitation mechanisms for Er^{3+} in GaN are applicable to other RE dopants in semiconductor hosts, we have extended the site-selective PL and PLE studies of RE excitation mechanisms to Nd-implanted GaN films grown by metal-organic chemical-vapor deposition (MOCVD). In this paper we report the observation of multiple, distinct ${}^4F_{3/2} \rightarrow {}^4I_{11/2}$ Nd^{3+} emission spectra characteristic of five different Nd^{3+} sites in the Nd-implanted GaN. The site-selective PLE spectra of these Nd^{3+} PL bands include broad, below-gap absorption bands that closely parallel those observed in the PLE of GaN:Er. The similarities and relationships between the Nd^{3+} and Er^{3+} PL and PLE spectra in GaN, the optical-absorption processes that selectively excite the five distinct Nd^{3+} sites, and the implications for the trap-mediated excitation mechanisms are discussed.

GaN films grown on (0001) sapphire by atmospheric pressure MOCVD were implanted with a dosage of 1×10^{14} ions/cm² at 320 keV, with a projected range of 0.06 μm for the implanted Nd ions. The implanted samples were annealed at 1000 °C for 90 min under a continuous flow of nitrogen gas.⁸ PLE and PL spectroscopies were carried out on the Nd-implanted GaN at 6 K. The PL spectra were excited by a variety of sources: the 819-nm line from a tunable titanium-doped sapphire laser, the 633-nm line from a HeNe laser, the 515- and 458-nm lines from an Ar-ion laser, 420-nm light from a xenon lamp, and the 325-nm line from a HeCd laser. The PLE spectra were obtained with a xenon lamp dispersed by a double-grating monochromator or with

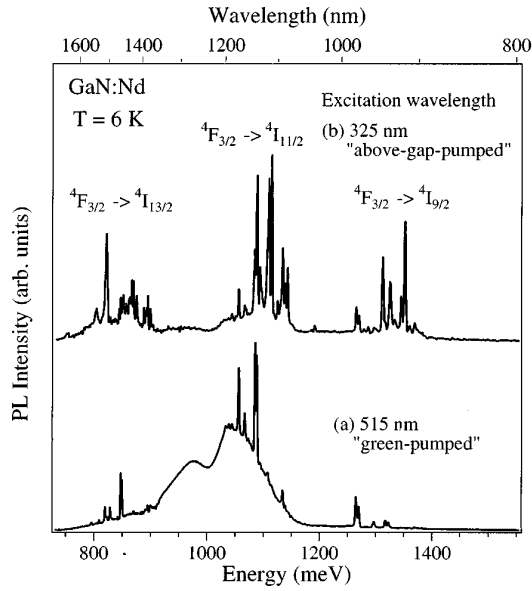


FIG. 1. PL spectra of the Nd-implanted GaN excited by a 515-nm line (a) and a 325-nm line (b). Both PL spectra exhibit three sharply structured emissions from the ${}^4F_{3/2} \rightarrow {}^4I_{9/2}$, ${}^4F_{3/2} \rightarrow {}^4I_{11/2}$, and ${}^4F_{3/2} \rightarrow {}^4I_{13/2}$ transitions of Nd^{3+} , which are superimposed on the broad damage-induced PL bands.

the tunable titanium-doped sapphire laser. All of the PLE spectra were corrected for the spectral response of the tunable excitation systems. The luminescence was analyzed by a 1-m single grating monochromator and detected by a cooled Ge *p-i-n* detector.

Figure 1 shows two PL spectra from the Nd-implanted MOCVD-grown GaN, one excited at 515 nm [Fig. 1(a)], and the other one excited by 325-nm above-gap light [Fig. 1(b)]. Both PL spectra exhibit three sharply structured emissions from the ${}^4F_{3/2} \rightarrow {}^4I_{9/2}$, ${}^4F_{3/2} \rightarrow {}^4I_{11/2}$, and ${}^4F_{3/2} \rightarrow {}^4I_{13/2}$ transitions of Nd^{3+} . These Nd^{3+} emissions are superimposed on the broad ion-implantation damage-induced PL bands reported in Refs. 3 and 8. The features of the PL spectrum excited by 515-nm light [Fig. 1(a)] are identical to those of the spectrum excited at 515 nm reported in Ref. 8 for Nd-implanted, MOCVD-grown GaN samples annealed at 1000 °C. However, the features of the above-gap excited PL spectrum [Fig. 1(b)] are more complicated than those of the 515-nm-excited spectrum [Fig. 1(a)]. A careful comparison of these two PL spectra reveals that the fine structure of the above-gap excited PL spectrum includes the dominant peaks observed in the 515-nm line excited PL spectrum, as well as additional peaks not present in the 515-nm-pumped spectrum. For example, the above-gap-pumped PL spectrum includes all the prominent peaks of the 515-nm-pumped PL spectrum (e.g., 980, 1142, and 1463 nm), but it also exhibits prominent peaks in the 916–944-, 1084–1112-, and 1375–1454-nm spectral ranges that are not observed in the 515-nm-pumped spectrum. This indicates that the above-gap excited PL spectrum could be a mixture of PL spectra associated with multiple Nd^{3+} sites which might be excited selectively by different below-gap optical-absorption processes, as observed for Er-implanted GaN.^{4–7}

PLE spectroscopy was performed on several PL peaks selected from the ${}^4F_{3/2} \rightarrow {}^4I_{11/2}$ transitions of Nd^{3+} in the above-gap excited PL spectrum of Fig. 1(b). Figure 2 dis-

plays five distinctly different PLE spectra obtained by detecting at the Nd^{3+} emission wavelengths marked by arrows in the high resolution PL spectra presented in Fig. 3. In addition, the PLE spectrum detected at the ~ 1.04 -eV peak position of the highest intensity in the broadband damage-induced emission [Fig. 1(a)] is shown in Fig. 2(f) for comparison. The PLE spectrum [Fig. 2(a)] obtained in the 794–824-nm spectral range with the tunable Ti-doped sapphire laser detecting at the wavelength marked by the arrow labeled *a* in Fig. 3 exhibits sharp-line PLE peaks assigned to direct Nd^{3+} ${}^4I_{9/2} \rightarrow {}^4F_{5/2} + {}^4H_{9/2}$ *4f*-shell absorption.⁹ The PLE spectra [Figs. 2(b), 2(c), and 2(d)] obtained with a xenon lamp reveal distinctive broad, below-gap absorption bands marked by arrows in the PLE spectra at 1.95, 2.75, and 3.0 eV, respectively. A strong absorption band at ~ 2.35 eV and a weak absorption band at ~ 1.8 eV seen in each of these PLE spectra are attributed to damage-induced absorption characteristic of the implanted films.⁷ The energy positions of the absorption bands in the PLE spectra [Figs. 2(b) and 2(c)] are close to those in the absorption bands of the PLE spectra previously observed in both Er-implanted GaN and the Cr-implanted GaN control sample discussed in Ref. 4. This indicates that the same defects (or impurities) characteristic of the as-grown GaN films are involved in the site-selective excitation of both the Er^{3+} and Nd^{3+} sites. The differences between the broadband PLE spectra for the two materials are attributable to the larger degree of spectral overlap among the PL spectra from the various Er^{3+} sites than there is for the Nd^{3+} sites, and the fact that the Er^{3+} and Nd^{3+} PL spectra overlap different portions of the underlying broad defect PL bands which contribute their own broad PLE bands.

The absorption band peaking at ~ 3.0 eV in the below-gap PLE [Fig. 2(d)] is attributed to defects created by Nd itself; a similar Er-related PLE band was observed previously in Er-implanted GaN,^{4,7} but its energy position is higher by ~ 0.1 eV. The PLE spectrum [Fig. 2(e)] does not show any significant below-gap absorption band (except damage-induced absorption bands peaking at ~ 2.35 and ~ 1.8 eV), but a relatively strong above-gap absorption band. The five different PLE spectra of Figs. 2(a), 2(b), 2(c), 2(d), and 2(e) exhibit five different excitation mechanisms for the Nd^{3+} sites in Nd-implanted GaN.

Figure 3 shows the ${}^4F_{3/2} \rightarrow {}^4I_{11/2}$ Nd^{3+} emission spectra selectively excited from Nd-implanted GaN by five different pump wavelengths corresponding to different absorption processes and excitation mechanisms. A sharp-line *4f* PLE peak (819 nm), red (633 nm), blue (458 nm), and violet (420 nm) light [the exciting wavelengths marked by arrows in the inset of Fig. 2 and in Figs. 2(b), 2(c), and 2(d), respectively] were used to pump the PL spectra of Figs. 3(a), 3(b), 3(c), and 3(d), respectively. These *4f*-, red-, blue-, and violet-pumped Nd^{3+} PL spectra each contain sets of distinctively prominent peaks. The red- and blue-pumped Nd^{3+} PL peaks dominate the above-gap excited Nd^{3+} PL spectrum [Fig. 3(e)], while the violet- and *4f*-pumped Nd^{3+} PL spectra are barely observable. However, the above-gap excited PL spectrum also contains strong peaks at wavelengths that do not correspond to the peaks that are characteristic of the four below gap excited PL spectra. These additional peaks are strongly excitable only by above-gap light (see the PLE

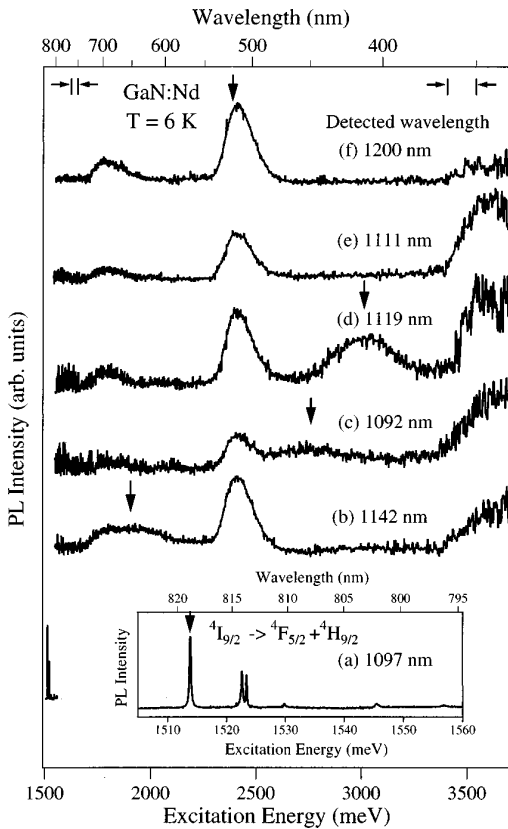


FIG. 2. Five different PLE-spectra (a), (b), (c), (d), and (e) detected at five different wavelengths indicated by *a*, *b*, *c*, *d*, and *e*, respectively, in Fig. 3(e); the PLE spectrum (f) detected at the peak position of the highest intensity in the damage-induced emission in Fig. 1(a) is shown for comparison. The sharp 4*f*-shell PLE spectrum pumped by the tunable cw Ti:sapphire laser in the ${}^4I_{9/2} \rightarrow {}^4F_{5/2} + {}^4H_{9/2}$ Nd^{3+} 4*f*-shell bands is shown in the inset. The five detected wavelengths marked in the Fig. 3(e) correspond to the most prominent peaks in the five different site-selective PL spectra in Fig. 3.

spectrum [Fig. 2(e)]. These five different groups of the dominant PL peaks apparently illustrate the existence of at least five distinct Nd^{3+} sites in the Nd-implanted GaN.

Four of the five different Nd^{3+} sites existing in the Nd-implanted GaN can be selectively excited by three different below-gap optical-absorption processes: (1) unidentified impurity- or defect-related absorption bands, (2) an absorption band associated with a Nd-related defect or trap, and (3) direct, sharp-line Nd^{3+} intra-4*f*-shell absorption bands. These four sites are also excited by above-gap light. These below- and above-gap excitation mechanisms of the four Nd^{3+} sites are also observed for the four Er^{3+} sites in Er-implanted samples of the same MOCVD GaN, as evidenced by the close similarity between the Nd^{3+} PLE spectra of Fig. 2, and those reported previously for the four Er^{3+} PL spectra.⁴⁻⁷ The fifth Nd^{3+} site is not efficiently pumped by below-gap light, but it is strongly excited by above-gap light. Although a fifth Er^{3+} site was not observed in our previously reported studies of site-selective PL and PLE in Er-implanted GaN,⁷ careful re-examination of the above-gap excited Er^{3+} PL spectra in GaN samples annealed at various temperatures clearly reveals the existence of a fifth Er^{3+} site.¹⁰

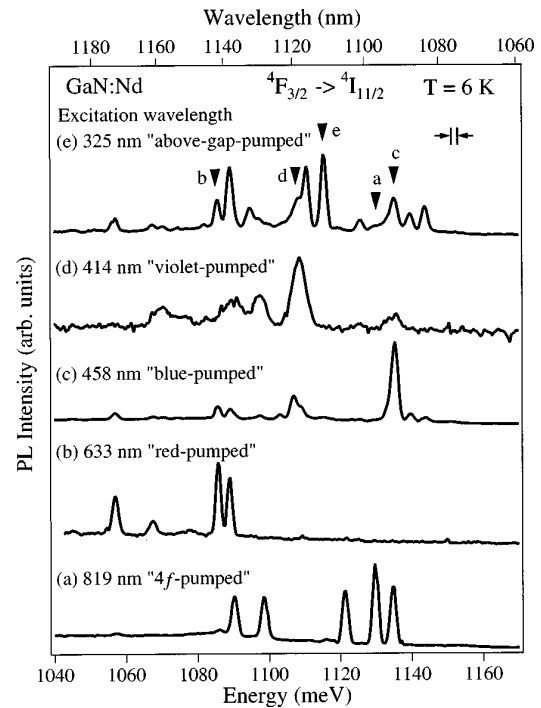


FIG. 3. Comparison among the crystal field split ${}^4F_{3/2} \rightarrow {}^4I_{11/2}$ intra-4*f*-shell emissions of Nd^{3+} in the 6-K PL spectra site, selectively pumped by (a) a sharp line 4*f* PLE peak (819 nm, 40 mW), (b) red (633 nm, 5 mW), (c) blue (458 nm, 40 mW), (d) violet (420 nm, 30 μW), and (e) above-gap (325 nm, 3 mW) light. The 4*f*, red, blue, violet, and above-gap-pumped Nd PL spectra are characterized by their most prominent peaks at 1097, 1142, 1092, 1119, and 1111 nm, respectively.

The parallel observations of five distinct Nd^{3+} and Er^{3+} sites in Nd- and Er-implanted GaN, respectively, and the obvious similarities of the site-selective PLE spectra obtained for these sites in both materials, clearly indicate that the distinctive absorption bands in the PLE spectra are defect- or impurity-related absorptions that are characteristic of either the as-grown films or implantation-induced defects in the films, and they are not attributable to absorption by the rare earths (e.g., direct 4*f*-shell excitation) which would be different for Er^{3+} and Nd^{3+} . Apparently, the defects or impurities giving rise to the “red,” “blue,” and 2.35-eV site-selective PLE bands also perturb the crystal field at neighboring Nd^{3+} or Er^{3+} sites, and induce the unique, site-selective spectral distributions of the Er^{3+} and Nd^{3+} emissions. Only in the case of the “violet” PLE band, whose peak energy differs slightly for the two different rare earths, is the rare-earth atom believed to play a direct role in the absorption by forming an isoelectronic trap that binds an exciton.

The most probable locations for the implanted Nd atoms in the GaN crystal include substitutional sites on the Ga sublattice, and interstitial sites. For wurtzite GaN, all the Ga atoms occupy sites of symmetry C_{3v} ,¹¹ and two distinct high-symmetry interstitial positions in the wurtzite crystal lattice also have C_{3v} symmetry.¹² For a Nd atom located on any of these C_{3v} sites, the Nd^{3+} PL spectrum corresponding to transitions from the ground state level of the ${}^4F_{3/2}$ manifold to the crystal-field-split ${}^4I_{11/2}$ manifold should exhibit six zero-phonon lines.^{2,13} However, the same is true for Nd^{3+}

located on any other noncubic site in the crystal, so the Nd^{3+} PL spectra cannot provide an identification of the lattice site. In the $4f$ -pumped Nd^{3+} PL spectrum shown in Fig. 3(a), five prominent peaks are clearly seen, but there is no obvious sign of a sixth peak.

On the basis of the work of Ronning *et al.*,¹⁴ who demonstrated that In atoms in In-implanted GaN are substituted on Ga sites, it is suggested that substitutional Ga sites (as opposed to interstitial sites) are the most likely location for the implanted Er and Nd in GaN. In addition, it is concluded that since only one of the distinct rare-earth sites in both Er- and Nd-implanted GaN exhibits a sharp-line PLE spectrum characteristic of direct $4f$ -band absorption, that site must be present in a significantly higher concentration than the other sites. This conclusion, which was first made in our previous work on Er-implanted GaN,^{6,7} is based on the fact that the cross section for absorption by intra- $4f$ shell transitions in rare-earth atoms is quite small ($\sim 10^{-21}$ cm²), and a large concentration of a particular rare earth site is therefore required for direct intra- $4f$ shell PLE. Furthermore, because these highest concentration sites exhibited no broadband PLE due to closely associated impurities or defects (as do the other distinct rare-earth sites), it is suggested that the high concentration rare earth sites might be rare-earth atoms on isolated Ga sites (i.e., they have no closely associated impurities or defects).

In the $4f$ -pumped PL spectrum of Fig. 3(a), the dominant highest-energy Nd^{3+} peak (arising from the transition of the ground level of the $^4F_{3/2}$ manifold to the ground level of $^4I_{11/2}$ manifold) is observed at 1093 nm. This wavelength position is very close to the wavelengths (~ 1090 nm) of the corresponding peaks observed for both GaAs:Nd (Ref. 2) and GaP:Nd.^{2,3} In contrast, no strong peaks are observed near 1090 nm in the red-, violet-, and above-gap-pumped Nd^{3+} PL spectra, and the highest-energy position Nd^{3+} peak in the blue-pumped Nd^{3+} PL spectrum is not strongly excited. Furthermore, the positions of the dominant peaks in

the red-, violet-, and above-gap-pumped Nd^{3+} PL spectra are significantly different from that in the $4f$ -pumped Nd^{3+} PL spectrum. These observations are consistent with our previous suggestion that the defects involved in the excitations of those four Nd^{3+} PL spectra may influence the local structural environment surrounding the substitutional Nd^{3+} ion on the Ga site, thereby affecting both the strengths of the optical transitions (of the ground level of the $^4F_{3/2}$ manifold to the $^4I_{11/2}$ manifold) and the energy positions of the levels of the $^4F_{3/2}$ and $^4I_{11/2}$ manifolds. Because of the perturbing influence of neighboring defects or impurities, the four Nd^{3+} sites responsible for these four Nd^{3+} PL spectra may have symmetries lower than C_{3v} . However, it is not possible to determine this from the Nd^{3+} PL spectra.

In summary, site-selective PL and PLE spectroscopies reveal the presence of five distinct Nd^{3+} sites in our Nd-implanted MOCVD-grown GaN crystal. Four of the five Nd^{3+} sites are excitable at varying efficiencies by above-gap light, and by three independent, site-selective below-gap absorption processes. A fifth Nd^{3+} site is strongly excited only by above-gap light. The below-gap excitation processes include direct sharp-line Nd^{3+} $4f$ -shell absorption, and broad, below-gap absorption bands attributable to defects and impurities and a possible isoelectronic trap associated with one of the five Nd^{3+} sites. It is concluded that the Nd^{3+} site that is excited by direct sharp-line Nd^{3+} $4f$ -shell absorption is the dominant or highest concentration Nd^{3+} center. The above-gap and broadband below-gap excitation mechanisms all involve the nonradiative transfer of energy from impurity- or defect-related traps to neighboring rare-earth atoms. It is suggested that these trap-mediated excitation processes control the thermal quenching of rare-earth emissions in rare-earth-doped semiconductors.

This work was supported by the NSF under the Engineering Research Centers Program (ECD 89-43166), DARPA (MDA972-94-1-004), and the JSEP (0014-90-J-1270).

¹R. A. Hogg *et al.*, J. Appl. Phys. **79**, 8682 (1996); K. Takahei and A. Taguchi, *ibid.* **77**, 1735 (1995).

²H. D. Muller *et al.*, J. Appl. Phys. **79**, 2210 (1986); J. Wagner *et al.*, *ibid.* **79**, 1202 (1986).

³K. Takahei and H. Nakagome, J. Appl. Phys. **72**, 3674 (1992).

⁴S. Kim *et al.*, Appl. Phys. Lett. **71**, 231 (1997).

⁵S. Kim *et al.*, Appl. Phys. Lett. **71**, 2662 (1997).

⁶S. Kim *et al.*, in *Gallium Nitride and Related Materials II*, edited by C. R. Abernathy, H. Amano, and J. C. Zolper, MRS Symposium Proceedings No. 468 (Materials Research Society, Pittsburgh, 1997), p. 131.

⁷S. Kim *et al.*, J. Electron. Mater. **27**, 246 (1998).

⁸E. Silkowski *et al.*, in *Rare-Earth Doped Semiconductors*, edited by A. Polman, S. Cotton, and R. Schwartz, MRS Symposia Proceedings No. 422 (Materials Research Society, Pittsburgh, 1996), p. 69.

⁹R. Beach *et al.*, IEEE J. Quantum Electron. **26**, 1405 (1990).

¹⁰S. Kim *et al.* (unpublished).

¹¹A. Clingolani *et al.*, Solid State Commun. **58**, 823 (1986).

¹²P. Boguslawski *et al.*, Phys. Rev. B **51**, 17 255 (1995).

¹³A. A. Kaminskii, *Laser Crystals: Their Physics and Properties* (Springer-Verlag, Berlin, 1990), p. 120.

¹⁴C. Ronning *et al.*, in *Gallium Nitride and Related Materials II* (Ref. 6), p. 407.